Building Simulation 2005

Ninth International IBPSA Conference
Montréal, Canada
August 15-18, 2005

A PROPOSED SYSTEM-LEVEL MODEL FOR SIMULATING THE THERMAL AND ELECTRICAL PRODUCTION OF SOLID-OXIDE FUEL CELL RESIDENTIAL COGENERATION DEVICES WITHIN WHOLE-BUILDING SIMULATION

Ian Beausoleil-Morrison [1], Adrian Schatz [2], François Maréchal [3]

[1] CANMET Energy Technology Centre, Natural Resources Canada, Ottawa Canada (ibeausol@nrcan.gc.ca)
[2] Sulzer Hexis Ltd., Winterthur Switzerland (Adrian.Schatz@sulzer.com)
[3] Swiss Federal Institute of Technology (EPFL), Lausanne Switzerland (francois.marechal@epfl.ch)

ABSTRACT

A new model for predicting the thermal and electrical performance of solid-oxide fuel cell (SOFC) cogeneration devices for residential buildings has been developed. This is a system-level model that considers the thermodynamic performance of all components that consume energy and produce the SOFC-cogeneration device's thermal and electrical output. The model relies heavily upon empirical information that can be acquired from the testing of coherent systems or components and is designed for operation at a time resolution that is in the order of minutes. Hence it is appropriate for use in whole-building simulation programs where it can be applied to assess the energy and greenhouse gas emissions benefits of this nascent technology.

INTRODUCTION

Residential cogeneration is an emerging technology with a high potential to deliver energy services with increased efficiency and environmental benefits. The concurrent production of electricity and heat from a single fuel source can reduce primary energy consumption and associated greenhouse gas (GHG) emissions. Reductions in combustion by-products such as nitrogen oxides and hydrocarbons are also a possibility. The decentralized production of electricity also has the potential to reduce electrical transmission and distribution congestion and to alleviate utility peak demand problems. A number of manufacturers worldwide are developing residential-scale cogeneration devices based upon fuel cells, internal combustion engines, and Stirling cycles (Knight and Ugursal 2005).

The effective exploitation of the cogeneration device's thermal output for space heating, space cooling, and/or heating domestic hot water (DHW) is critical to realizing high levels of overall energy efficiency and the associated environmental benefits. Consequently, the performance of these devices will be highly dependent upon how the cogeneration device is integrated to service the host building's thermal and electrical demands. In order to accurately assess performance, therefore, it is imperative that models of cogeneration devices be incorporated into whole-building simulation tools that account for the interactions between the building and its environment, the occupants, the thermal and electrical production and distribution systems, and energy management and control systems.

These factors motivated the formation of Annex 42 of the International Energy Agency's Energy Conservation in Buildings and Community Systems Programme (IEA/ECBCS)[1]. This international collaborative project aims to develop, validate, and implement models of cogeneration devices for whole-building simulation programs.

This paper describes the mathematical model that IEA/ECBCS Annex 42 is developing for simulating the performance of solid oxide fuel cell (SOFC) cogeneration devices within whole-building simulation programs. This model is based upon the earlier work of Beausoleil-Morrison et al (2002) and the modelling experiences of Sulzer-Hexis and other IEA/ECBCS Annex 42 participants.

SOFC COGENERATION

Fuel cells are energy conversion devices that directly convert chemical energy to electrical energy. This is accomplished through the electrochemical oxidation of a fuel and the electrochemical reduction of oxygen. These electrochemical reactions occur at electrodes which are continuously fed with fuel and oxygen and which are separated by an electrolyte layer.

SOFCs use a solid metal oxide as the electrolyte. These show particular promise for residential cogeneration applications because of their high operating temperature (600 to 1 000^oC) and their ability to operate directly on natural gas. These temperatures are sufficient to internally reform the gas' constituent hydrocarbon molecules (methane, ethane, propane, etc.) to hydrogen and carbon monoxide which are then supplied to the electrode where they are partially oxidized with the oxygen crossing the electrolyte. Internal reforming avoids either the need to deliver and store hydrogen at the building site, or the cost, energy, and space requirements of an external fuel reformer. The second advantage of the SOFC's high operating temperature is the production of thermal energy at temperatures that can be exploited for space heating, space cooling, and/or DHW heating.

[1] The Annex's web site is www.cogen-sim.net.

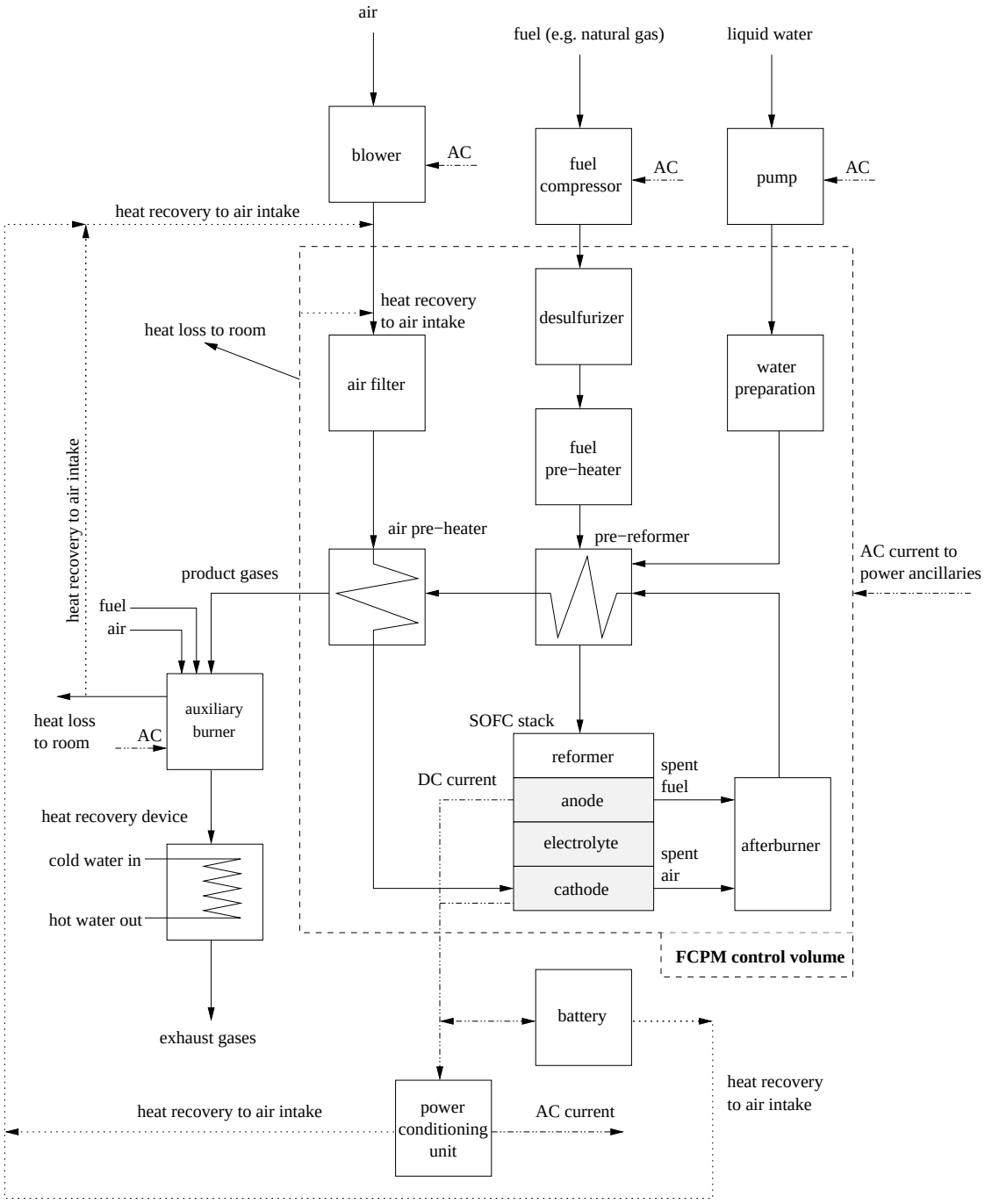

Figure 1: One possible system configuration of a SOFC-cogeneration device

The interested reader is referred to Singhal and Kendall (2003) for a thorough review of SOFC technology and to Ellis and Gunes (2002) for a discussion on the use of fuel cells for building cogeneration.

It is important to note that the fuel cell stack itself is only a single component within a complex energy conversion system. Figure 1 illustrates one possible system configuration of a SOFC-cogeneration device. Besides the fuel cell stack (shown in grey), the system might include: an afterburner to combust unreacted fuel; an air filter and pre-heater; a fuel desulfurizer, pre-heater, pre-reformer, and reformer; and water preparation. A blower, a compressor, and a pump may be required for supplying air, fuel, and water to the system. A battery could be used for buffering the fuel cell stack's DC electrical production and for meeting load transients and the system will include a power conditioning unit to convert the electrical output to AC. All SOFC-cogeneration systems will include a heat recovery device that transfers the heat of the hot product gases to the building's plant system. Some systems may include an integrated auxiliary burner that is activated when the fuel cell cannot satisfy the building's thermal loads.

THE IEA/ECBCS ANNEX 42 MODEL

Many detailed SOFC models are presented in the literature. However, most of these are not well suited for the purposes of IEA/ECBCS Annex 42. Many of these models focus on single cells or stacks of cells while other components (refer to Figure 1) are left untreated (e.g. Beale et al 2003; Bove et al 2005).

In contrast, IEA/ECBCS Annex 42 requires a model that considers the thermodynamic performance of the complete system. This SOFC-cogeneration model will be coupled to models of associated plant components, such as hot-water storage, peak-load boilers and heaters, pumps that circulate hot or cold water from the plant to hydronic heaters located in the rooms or to air-handling units, fans that circulate conditioned air to the rooms, and heat exchangers. In turn, these models representing the building's coherent plant and electrical production systems will be coupled to models that predict the building's thermal and electrical demands.

Control volume representation

Eight control volumes are used to discretize the model of the SOFC-cogeneration system:

1) The fuel cell power module (FCPM) which includes the stack, the afterburner, and the other components enclosed by the dashed line in Figure 1.
2) The air supply blower.
3) The fuel supply compressor.
4) The water pump.
5) An auxiliary burner.
6) An exhaust-gas-to-water heat exchanger.
7) A battery system for electrical storage.
8) A DC-AC power conditioning unit.

The following sections describe some of the methods used for resolving the three control volumes that are most critical from the perspective of predicting the thermal and electrical production: the FCPM, the auxiliary burner, and the exhaust-gas-to-water heat exchanger. The interested reader is referred to Beausoleil-Morrison (2005) for a complete treatment of the model.

FUEL CELL POWER MODULE

As described above the FCPM control volume is drawn to encompass the fuel cell stack as well as a number of the balance of plant components. This is done for the following pragmatic reasons:

- Product-specific information regarding the arrangement of components is not required, an important consideration since many manufacturers consider this information to be proprietary.
- The model can represent SOFC's with indirect internal reforming (hydrocarbons are reacted to H_2 and CO at a catalyst that is physically separated but thermally coupled to the anode) or direct internal reforming (hydrocarbons are reacted at the anode).
- The model can represent both planar and tubular SOFC designs.
- Inputs to the model can be derived from empirical measurements made on either individual subsystems or from coherent system testing. Alternatively, the model inputs can be derived from highly detailed mechanistic subsystem modelling that is performed independently from the building simulation programs.

Energy balance

Referring Figure 1, the following energy balance can be written for the control volume representing the FCPM (the dashed line),

$$\dot{H}_{fuel} + \dot{H}_{air} + \dot{H}_{l-water} + P_{el,anc-AC} = P_{el} + \dot{H}_{FCPM-cg} + q_{skin-loss} \quad (1)$$

$\dot{H}_{fuel}$, $\dot{H}_{air}$, and $\dot{H}_{l-water}$ are the total enthalpy flow rates of the fuel, air, and liquid water introduced to the control volume. $\dot{H}_{FCPM-cg}$ is the total enthalpy flow rate of the product gases exiting the control volume and entering the auxiliary burner. $q_{skin-loss}$ represents the parasitic thermal losses in the form of radiation and convection to the containing room. P_{el} is the net DC electric power produced by the FCPM while $P_{el,anc-AC}$ is the power draw of the ancillaries that are included within the control volume and that are powered by AC electricity that is supplied to the cogeneration device. (All terms in equation 1 are expressed in units of W.)

The total enthalpy flow rates of the gas streams in equation 1 represent summations of the enthalpies of their constituent gases, e.g.

$$\dot{H}_{fuel} = \sum_i (\dot{N}_i \hat{h}_i)_{fuel} \quad (2)$$

Where $\hat{h}_i$ is the molar enthalpy (J/kmol) and $\dot{N}_i$ is the molar flow rate (kmol/s) of fuel constituent i (CH_4, C_2H_6, CO_2, N_2, etc).

For convenience, the enthalpy of each reactant or product gas is expressed as a sum of its enthalpy at the standard state (i.e. the standard enthalpy of formation) and the deviation between its enthalpy and that at the standard state,

$$\hat{h}_i = \Delta_f \hat{h}_i^o + \left[\hat{h}_i - \Delta_f \hat{h}_i^o \right] \quad (3)$$

Where $\Delta_f \hat{h}_i^o$ is the molar enthalpy of gas i at the standard state (J/kmol).

If it is assumed that the reactions of the fuel constituents are complete (a reasonable assumption given the high operating temperatures of the SOFC

stack and the afterburner, as confirmed by the emissions data given by Karakoussis et al 2000), then the fuel's lower heating value (LHV) can be conveniently introduced into the energy balance. The LHV (J/kmol) of a fuel is expressed using the standard enthalpies of formation of the reactants and products (see Reynolds and Perkins 1977, for example),

$$LHV_{fuel} = \frac{\Delta_f H^o_{fuel} - \Delta_f H^o_{CO_2} - \Delta_f H^o_{H_2O}}{\dot{N}_{fuel}} \quad (4)$$

Where $\Delta_f H^o_{fuel}$ is the total flow rate of the standard enthalpy of formation of the fuel entering the FCPM control volume and $\Delta_f H^o_{CO_2}$ and $\Delta_f H^o_{H_2O}$ are the total flow rates of the enthalpies of formation of the product gases created by the complete reaction of the fuel (all in W). $\dot{N}_{fuel}$ is the molar flow rate of the fuel (kmol/s).

The FCPM's electrical efficiency is expressed relative to the fuel's LHV

$$\varepsilon_{el} = \frac{P_{el}}{\dot{N}_{fuel} \cdot LHV_{fuel}} \quad (5)$$

By substituting equations 2 through 5 into equation 1 and rearranging, the energy balance on the FCPM can be expressed as,

$$\sum_i (\dot{N}_i \cdot [\hat{h}_i - \Delta_f \hat{h}^o_i])_{fuel} + \sum_i (\dot{N}_i \cdot [\hat{h}_i - \Delta_f \hat{h}^o_i])_{air} \quad (6)$$

$$+ H_{l-water} + P_{el,anc-AC} + (1 - \varepsilon_{el}) \cdot \dot{N}_{fuel} \cdot LHV_{fuel}$$

$$= \sum_i (\dot{N}_i \cdot [\hat{h}_i - \Delta_f \hat{h}^o_i])_{FCPM-cg} + q_{skin-loss}$$

Electrical efficiency

It is common to model the electrochemical behaviour of fuel cell stacks by predicting cell voltages using the Nernst potential with empirical adjustments to account for activation, concentration, and ohmic losses (see, for example, Van herle et al 2004; Bove et al 2005). Such an approach requires methods to establish the stack temperature and stack fuel utilization efficiency. This can only be accurately accomplished with an a priori knowledge of the system configuration, operational controls, and heat transfer characteristics between individual components (see Chan and Ding 2005, for example).

In the IEA/ECBCS Annex 42 model the fuel cell stack has been grouped with other components such as the afterburner and heat exchangers into the FCPM control volume. Such a treatment avoids the complications discussed above but also precludes an explicit treatment of the fuel cell's electrochemical behaviour. Consequently, this model does not attempt to simulate the electrochemical processes occurring within the fuel cell, but rather represents the electrochemical performance of the FCPM using a parametric relation between the electrical efficiency and the net electrical power output,

$$\varepsilon_{el} = \left[\varepsilon_0 + \varepsilon_1 \cdot P_{el} + \varepsilon_2 \cdot P^2_{el}\right] \cdot \left[1 - N_{stops} \cdot D\right] \quad (7)$$

The $[1 - N_{stops} \cdot D]$ term in equation 7 represents the degradation of the FCPM's electrical efficiency as a result of stop-start cycling. (Electrical performance may degrade with time due to the thermal stresses induced during cool-down and warm-up). N_{stops} represents the number of times the SOFC-cogeneration system has been stopped and then restarted since its initiation and D is a user-input fixed value representing the fractional performance degradation associated with each cycle.

The approach represented by equation 7 provides a great deal of flexibility for characterizing a FCPM's electrochemical performance. The ε_i coefficients are supplied by the user. These coefficients could be determined by regressing measured data from a coherent system (as was done by Beausoleil-Morrison et al 2002). Alternatively, empirical or analytical models could be used to predict polarization curves for a given cell design, and additional models coupled to these to predict fuel utilization ratios and flow rates to produce a performance map that leads to the ε_i coefficients. Another option is to employ detailed multi-dimensional mechanistic electrochemical, flow, and energy models based upon numerical discretization and solution schemes to predict FCPM performance over a range of operating points and then parameterize the results to yield the ε_i coefficients. Examples of detailed models that could be used are those of Braun (2002) and Petruzzi et al (2003).

It is worth noting that the three options listed above for establishing the ε_i coefficients all rely heavily upon empirical data, either characterizing performance at the system level or at the molecular level.

Air supply to FCPM

The form of equation 7 that represents the electrochemical performance of the FCPM includes an implicit relationship between the fuel and air supply rates. The model therefore requires an explicit relationship. Three alternate methods are provided for specifying this relationship.

All three methods make use of an excess air ratio (λ) that is based upon the stoichiometric reactions of the fuel constituents,

$$C_x H_y O_z + \left(x + \tfrac{y}{4} - \tfrac{z}{2}\right) \cdot O_2 \rightarrow x \cdot CO_2 + \tfrac{y}{2} \cdot H_2O \quad (8)$$

Equation 8 is applied to each of the fuel constituents. These results are combined with the flow rates of the fuel constituents and the user-specified molar fractions for the composition of air to establish the stoichiometric air flow rate, $\dot{N}^s_{air}$.

With the first method, the user specifies a fixed excess air ratio (λ) and the air flow rate is determined as follows,

$$\dot{N}_{air} = (1 + \lambda) \cdot \dot{N}^{s}_{air} \qquad (9)$$

The user-specified molar fractions for the composition of air then lead to the solution of the flow rate of each air constituent (N_2, O_2, H_2O, etc.) for the time-step.

Alternatively, the user may specify the excess air ratio as a parametric function of either the fuel flow rate or the net electrical output, e.g.,

$$\lambda = \frac{(a_0 + a_1 \cdot \dot{N}_{fuel} + a_2 \cdot \dot{N}^2_{fuel})}{\dot{N}^{s}_{air}} - 1 \qquad (10)$$

Next, the Shomate equation (NIST 2003) is used to evaluate the difference between a gas' enthalpy and its standard enthalpy of formation as a polynomial function of its temperature,

$$\hat{h}_i - \Delta_f \hat{h}^o_i = A \cdot \left(\frac{T}{1\,000}\right) + \frac{B}{2} \cdot \left(\frac{T}{1\,000}\right)^2 \qquad (11)$$

$$+ \frac{C}{3} \cdot \left(\frac{T}{1\,000}\right)^3 + \frac{D}{4} \cdot \left(\frac{T}{1\,000}\right)^4 - E \cdot \left(\frac{T}{1\,000}\right) + F - H$$

The evaluation of the aforementioned steps completes the determination of the $\sum_i (\dot{N}_i \cdot [\hat{h}_i - \Delta_f \hat{h}^o_i])_{air}$ term of equation 6.

FCPM Product gases

As previously stated, it is assumed that the reaction of the fuel constituents are complete. Given this, the flow rate of CO_2 and H_2O that are produced by electrochemical oxidation (in the fuel cell stack) and combustion (in the afterburner) can be determined with equation 8. The flow rates of the other product gas constituents are determined by assuming that the inert fuel and air constituents (e.g. Ar and N_2) and the excess O_2 pass through the FCPM control volume unreacted. Having established the composition of the product gas stream, the Shomate equation (equation 11) is used to establish the $\sum_i (\dot{N}_i \cdot [\hat{h}_i - \Delta_f \hat{h}^o_i])_{FCPM-cg}$ term of equation 6.

AUXILIARY BURNER AND HEAT RECOVERY

The components that accomplish the SOFC-cogeneration device's thermal output are treated in this section.

Auxiliary burner

Some SOFC-cogeneration devices may contain an integrated auxiliary burner for providing back-up heating. The Sulzer-Hexis system, for example, contains an integrated auxiliary burner and a double-chamber heat exchanger (Diethelm 2004). The combustion gases from the FCPM are directed through one chamber of the heat exchanger and the exhaust gases from the auxiliary burner through the second chamber. The building's plant circulates water through the heat exchanger to extract energy from both gas streams concurrently.

Although some SOFC-cogeneration systems may be configured with double-chamber heat exchangers, this model treats the combustion gases from the FCPM and the exhaust gases from the auxiliary burner as a single stream. It is felt that this modelling artifact will accurately represent the heat transfer from the enthalpy flow of the two gas streams while providing the model with flexibility for resolving various design configurations. Additionally, the control volume representing the auxiliary burner can be nullified in the case of designs where the auxiliary heating is either not present or accomplished elsewhere in the plant system (e.g. a burner within a water storage tank).

A schematic representation of the auxiliary burner control volume is illustrated in Figure 2. The state points shown in the figure are used in the development that follows. The control volume is represented by two sections to facilitate the description of its mathematical model: a burner section and a mixing section.

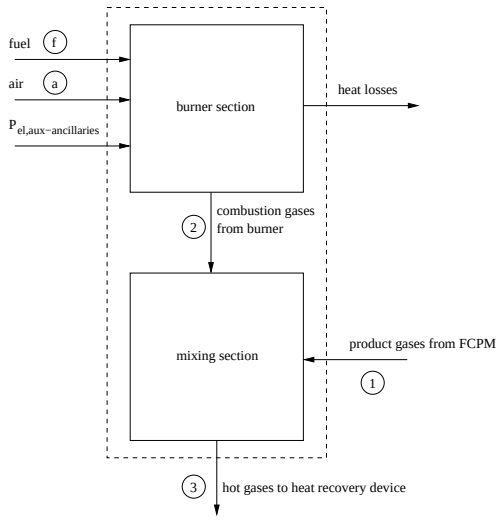

Figure 2: Auxiliary burner control volume

An energy balance can be written for the burner section that relates the total enthalpy flow rates of the supplied fuel and air and the exiting combustion gases, the heat losses from the burner, and the electrical power supplied to the burner's ancillary devices (all terms in units of W),

$$\dot{H}_f + \dot{H}_a + P_{el,aux-anc} = \dot{H}_2 + q_{aux-skin-loss} \qquad (12)$$

The flow rate of air introduced to the burner section (necessary for evaluating $\dot{H}_a$) is determined from the stoichiometric oxygen requirement (refer to equation 8) and from a constant user-specified

excess air ratio. The user can specify whether this air is drawn at the temperature of the room that contains the SOFC-cogeneration device or at the outdoor air temperature. (The fuel supply is treated in a similar manner.)

$P_{el,aux-anc}$ in equation 12 is the electrical power (W) supplied to the auxiliary burner's ancillary devices (e.g. combustion air supply fan, controls, ignition system). It is assumed that all of the electrical power supplied to these ancillaries is added to the control volume. A first-order expression is used to evaluate this term,

$$P_{el,aux-anc} = x_0 + x_1 \cdot \dot{N}_f \qquad (13)$$

Where $\dot{N}_f$ is the molar flow rate of the fuel mixture combusted in the auxiliary burner.

This formulation assumes that the ancillary power draws of the auxiliary burner are proportional to the burner's fuel supply rate with x_0 representing the consumption at the minimum allowable $\dot{N}_f$. (Note that $P_{el,aux-anc}$ is zero when the burner is inoperative.)

$q_{aux-skin-loss}$ in equation 12 is the heat loss (W) from the burner, that is the portion of the energy from the combustion of the fuel that does not leave the burner section in the gas stream (i.e. the $\dot{H}_2$ term). As shown in Figure 1, $q_{aux-skin-loss}$ can either be lost to the containing room or can be recovered to pre-heat the FCPM's air intake. It is assumed that this heat transfer is proportional to the temperature difference between the combustion gases exiting the burner section and the air in the room containing the SOFC-cogeneration device,

$$q_{aux-skin-loss} = (UA)_{aux} \cdot (T_2 - T_{room}) \qquad (14)$$

Where $(UA)_{aux}$ a heat loss coefficient supplied by the user (W/K) that characterizes the convection and radiation from the skin of the auxiliary burner to the containing room. T_{room} is the air temperature of the room (e.g. basement, garage). It is important to note that $(UA)_{aux}$ is not a function of the temperature difference between the surface of the auxiliary burner and the room air, but rather between the combustion gases and the room air. This is necessary as the placement of the control volume that represents the auxiliary burner precludes the explicit solution of its surface temperature. T_2 was selected as an appropriate reference temperature for the skin losses since there should be a correlation between it and the surface temperature.

By assuming that the combustion of the fuel is complete, the LHV of the fuel can be introduced into the energy balance (refer to previous development for the FCPM). With this, equation 12 can be represented by,

$$\sum_i (\dot{N}_i \cdot [\hat{h}_i - \Delta_f \hat{h}_i^o])_f + \sum_i (\dot{N}_i \cdot [\hat{h}_i - \Delta_f \hat{h}_i^o])_a \qquad (15)$$

$$+ P_{el,aux-anc} + \dot{N}_f \cdot LHV_f$$

$$= \sum_i (\dot{N}_i \cdot [\hat{h}_i - \Delta_f \hat{h}_i^o])_2 + q_{aux-skin-loss}$$

The enthalpy terms of equation 15 are evaluated using the Shomate equation and the methods elaborated for the treatment of the FCPM.

The burner's capacity is specified by the user and is expressed either in heat output (W) or fuel input (kmol/s). It is assumed that the burner can fully modulate from a minimum (user-specified) output to full capacity and that its operating point is controlled by a signal originating elsewhere in the plant system, e.g. a water storage tank temperature or the temperature of water returned from space-heating radiators.

Referring to Figure 2 and assuming that the control volume is adiabatic, molar and energy balances can be written for the mixing section as follows,

$$\dot{N}_{1,i} + \dot{N}_{2,i} = \dot{N}_{3,i} \qquad (16)$$

$$\sum_i (\dot{N}_i \cdot [\hat{h}_i - \Delta_f \hat{h}_i^o])_1 + \sum_i (\dot{N}_i \cdot [\hat{h}_i - \Delta_f \hat{h}_i^o])_2 \qquad (17)$$

$$= \sum_i (\dot{N}_i \cdot [\hat{h}_i - \Delta_f \hat{h}_i^o])_3$$

Where equation 16 applies for each constituent gas i, e.g. CO_2, H_2O, N_2.

The three terms in equation 17 represent the enthalpy flow rates relative to the standard state (W) of the gases exiting the FCPM control volume and the burner section and of the gases exiting the auxiliary burner control volume and entering the gas-side of the heat recovery device.

As previously stated, the auxiliary heater control volume can be easily nullified in the case of modelling SOFC-cogeneration systems where the auxiliary heating is either not present or accomplished elsewhere in the plant system. In this case equations 12 through 17 will reduce to a form that represents a flow-through control volume in which the flow rate and enthalpy of the gases exiting equal to the entering values.

Exhaust gas to water heat exchanger

A schematic representation of the control volume encapsulating the device that transfers heat from the auxiliary burner (or FCPM) control volume exhaust gases to the water loop connected to the building's plant is shown in Figure 3. The state points shown in the figure are used in the development that follows.

The heat transfer from the hot gases to the water is characterized with the log mean temperature difference (LMTD) method for counterflow heat exchangers,

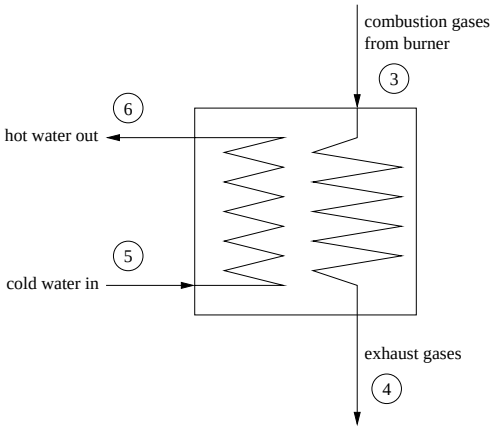

Figure 3: Heat exchanger control volume

$$q_{HX} = (UA)_{eff} \cdot \frac{(T_3 - T_6) - (T_4 - T_5)}{\ln\left(\frac{T_3 - T_6}{T_4 - T_5}\right)} \qquad (18)$$

Where T_4 is the temperature of the cooled gases that are exhausted to the ambient and T_6 is the temperature of the warmed water exiting the heat exchanger.

If it is assumed that heat loss from the heat exchanger to the ambient is negligible and that the heat capacity of each fluid stream remains constant through the heat exchanger, then the following energy balance can be written for the heat transfer between the fluid streams,

$$q_{HX} = (\dot{N}\hat{c}_P)_3 \cdot (T_3 - T_4) = (\dot{N}\hat{c}_P)_5 \cdot (T_6 - T_5) \qquad (19)$$

Equation 19 can be rearranged to express the outlet water temperature as a function of the water inlet temperature and the gas temperatures,

$$T_6 = T_5 + \frac{(\dot{N}\hat{c}_P)_3}{(\dot{N}\hat{c}_P)_5} \cdot (T_3 - T_4) \qquad (20)$$

By substituting equation 20 into the numerator of equation 18 and by replacing q_{HX} with $(\dot{N}\hat{c}_P)_3 \cdot (T_3 - T_4)$, it can be shown that,

$$\ln\left(\frac{T_3 - T_6}{T_4 - T_5}\right) = \frac{(UA)_{eff}}{(\dot{N}\hat{c}_P)_3} \cdot \left[1 - \frac{(\dot{N}\hat{c}_P)_3}{(\dot{N}\hat{c}_P)_5}\right] \qquad (21)$$

By taking the exponential of each side of equation 21, substituting in equation 20, and rearranging, the gas outlet temperature can be expressed as a function of gas and water inlet temperatures,

$$T_4 = \left\{ \frac{1 - \frac{(\dot{N}\hat{c}_P)_3}{(\dot{N}\hat{c}_P)_5}}{e^{\left[(UA)_{eff} \cdot \left(\frac{1}{(\dot{N}\hat{c}_P)_3} - \frac{1}{(\dot{N}\hat{c}_P)_5}\right)\right]} - \frac{(\dot{N}\hat{c}_P)_3}{(\dot{N}\hat{c}_P)_5}} \right\} \cdot T_3 \qquad (22)$$

$$+ \left\{ \frac{e^{\left[(UA)_{eff} \cdot \left(\frac{1}{(\dot{N}\hat{c}_P)_3} - \frac{1}{(\dot{N}\hat{c}_P)_5}\right)\right]} - 1}{e^{\left[(UA)_{eff} \cdot \left(\frac{1}{(\dot{N}\hat{c}_P)_3} - \frac{1}{(\dot{N}\hat{c}_P)_5}\right)\right]} - \frac{(\dot{N}\hat{c}_P)_3}{(\dot{N}\hat{c}_P)_5}} \right\} \cdot T_5$$

With the LMTD approach the effective heat transfer coefficient must be evaluated at each time-step of the simulation. Two optional methods are provided for evaluating $(UA)_{eff}$. The first employs an empirical approach which casts $(UA)_{eff}$ as a parametric relation with the water and product gas flow rates,

$$(UA)_{eff} = hx_{s,0} + hx_{s,1} \cdot \dot{N}_5 + hx_{s,2} \cdot \dot{N}_5^2 \qquad (23)$$

$$+ hx_{s,3} \cdot \dot{N}_3 + hx_{s,4} \cdot \dot{N}_3^2$$

This method can be particularly useful when empirical data are available from the testing of a specific heat exchange device over a range of water inlet and product gas temperatures and flow rates. Such experimental data can be easily regressed to provide the $hx_{s,i}$ coefficients. It is worth noting the empirical form of equation 23 compensates for some of the assumptions inherent to the LMTD method, namely that there is no heat loss from the heat exchanger, that perfect counterflow conditions prevail, and that the fluid heat capacities are constant throughout the heat exchanger.

With the second method $(UA)_{eff}$ is cast in an idealized form based upon more fundamental heat transfer processes,

$$(UA)_{eff} = \qquad (24)$$

$$\left[\frac{1}{(h^0 A)_{gas}\left(\frac{\dot{N}_3}{\dot{N}_3^0}\right)^n} + \frac{1}{(h^0 A)_{water}\left(\frac{\dot{N}_5}{\dot{N}_5^0}\right)^m} + F_{HX}\right]^{-1}$$

Where h_j^0 is the coefficient for the heat transfer from the heat exchanger surface to the air or gas stream at the nominal flow rate $\dot{N}_j^0$. These empirical constants as well as the empirical constants n and m are supplied by the user. The user also supplies reference heat exchanger areas A_j and the empirical constant F_{HX}, which is an adjustment factor to compensate for the errors inherent in the assumptions of equation 24 (e.g. that the wall temperatures of the heat exchanger are uniform) and those of the LMTD method.

To facilitate the analysis of hypothetical systems where the performance characteristics of the heat transfer device are unknown the user is given the option of supplying a fixed heat exchanger effectiveness (ε_{HX}). At each time-step of the simulation this is used to calculate the heat recovery based upon

the approach temperature, that is the temperature difference between the entering gas and water streams,

$$q_{HX} = \varepsilon_{HX} \cdot (\dot{N}\hat{c}_P)_{\min} \cdot (T_3 - T_5) \qquad (25)$$

Where $(\dot{N}\hat{c}_P)_{\min}$ is the minimum value of $(\dot{N}\hat{c}_P)_3$ and $(\dot{N}\hat{c}_P)_5$ for the current time-step.

Work is also underway on a method for resolving cases where water vapour in the exhaust gases condenses within the heat exchanger.

CONCLUDING REMARKS

The paper has provided a succinct summary of the SOFC-cogeneration model that is under development by IEA/ECBCS Annex 42. This is a system-level model that considers the thermodynamic performance of all components that consume energy and produce the SOFC-cogeneration device's thermal and electrical output.

This model is appropriate for use in whole-building simulation programs where it can be coupled to models of associated plant components (e.g. hot-water storage, hydronic heating systems, thermally activated cooling systems) and models that predict the building's thermal and electrical demands. Only by considering these interactions between the building thermal, plant, electrical, and generation domains can simulation accurately assess the potential energy and GHG emissions benefits of this nascent technology.

The SOFC-cogeneration model described in this paper is currently being implemented into the ESP-r (ESRU 2002) and EnergyPlus (Crawley et al 2001) simulation programs. It is expected that testing and analysis with these initial implementations will lead to model refinements and enhancements. Furthermore, IEA/ECBCS Annex 42 is conducting a programme of experimental work that will result in a suite of empirical and inter-program comparative tests that will be used to validate and improve the model.

Future papers will report these model enhancement and validation efforts as well as the simulation results obtained with the new models.

REFERENCES

Beale S.B., Lin Y., Zhubrin S.V., and Dong W. (2003), 'Computer Methods for Performance Prediction in Fuel Cells', *J. Power Sources* (118) 79-85.

Beausoleil-Morrison I., Cuthbert D., Deuchars G., and McAlary G. (2002), 'The Simulation of Fuel Cell Cogeneration Systems within Residential Buildings', *Proc. eSim 2002* 40-47, Montréal Canada.

Beausoleil-Morrison I. (2005), 'Model Specifications for an SOFC-Cogeneration Device', *IEA/ECBCS Annex 42 Working Document*.

Bove R., Lunghi P., and Sammes N.M. (2005), 'SOFC Mathematical Model for Systems Simulations. Part 1: From a Micro-Detailed to Macro-Black-Box Model', *Int J Hydrogen Energy* (30) 181-187.

Braun R.J. (2002), *Optimal Design and Operation of Solid Oxide Fuel Cell Systems for Small-Scale Stationary Applications*, Ph.D. Thesis, University of Wisconsin-Madison, USA.

Chan S.H. and Ding O.L. (2005), 'Simulation of a Solid Oxide Fuel Cell Power System Fed by Methane', *Int J Hydrogen Energy* (30) 167-179.

Crawley D.B., Lawrie L.K., Winkelmann F.C., Buhl W.F., Huang Y.J., Pedersen C.O., Strand R.K., Liesen R.J., Fisher D.E., Witte M.J., and Glazer J. (2001) 'EnergyPlus: Creating a New-Generation Building Energy Simulation Program', *Energy and Buildings* (33) 319-331.

Diethelm R. (2004), 'Cheaper, Compacter, and Lighter Through Greater System Integration', *Sulzer Technical Review* 4/2004.

Ellis M.W. and Gunes M.B. (2002), 'Status of Fuel Cell Systems for Combined Heat and Power Applications in Buildings', *ASHRAE Transactions*, AC-02-18-2.

ESRU (2002), *The ESP-r System for Building Energy Simulations: User Guide Version 10 Series*, ESRU Manual U02/1, University of Strathclyde, Glasgow UK.

Karakoussis V., Leach M., van der Vorst R., Hart D., Lane J., Pearson P., and Kilner J. (2000), *Environmental Emissions of SOFC and SPFC System Manufacture and Disposal*, Report F/01/00164/REP to British Department of Trade and Industry.

Knight I. and Ugursal V.I. (2005), 'Residential Cogeneration Systems: A Review of the Current Technologies', *IEA/ECBCS Annex 42 Report*.

NIST (2003), *Chemistry WebBook*, National Institute of Standards and Technology Standard Reference Database Number 69, March 2003 Release, http://webbook.nist.gov/chemistry/.

Petruzzi L., Cocchi S., Fineschi F. (2003), 'A Global Thermo-Electrochemical Model for SOFC Systems Design and Engineering', *Journal of Power Sources*, 118, 96-107.

Reynolds W.C. and Perkins H.C. (1977), *Engineering Thermodynamics*, McGraw-Hill.

Singhal S.C. and Kendall K. (2003), *High Temperature Solid Oxide Fuel Cells: Fundamentals, Design, and Applications*, Elsevier, Oxford UK.

Van herle J., Maréchal F., Leuenberger S., Membrez Y., Bucheli O., and Favrat D. (2004), 'Process Flow Model of Solid Oxide Fuel Cell System Supplied with Sewage Biogas', *J. Power Sources* (131) 127-141.